

APPENDIX MATERIAL FOR:

Notch Signaling Regulates Gastric Antral LGR5 Stem Cell Function

Elise S. Demitrack¹, Gail B. Gifford¹, Theresa M. Keeley¹, Alexis J. Carulli¹, Kelli L. VanDussen², Dafydd Thomas³, Thomas J. Giordano^{3,4}, Zhenyi Liu⁵, Raphael Kopan⁶, Linda C. Samuelson^{1,4}

Departments of ¹Molecular & Integrative Physiology, ³Pathology and ⁴Internal Medicine, The University of Michigan Medical School, Ann Arbor, MI 48109, USA.

Departments of ²Pathology and Immunology, ⁵Developmental Biology, Washington University School of Medicine, St. Louis, MO 63130

⁶Division of Developmental Biology, Cincinnati Children's Hospital Medical Center, University of Cincinnati College of Medicine, Cincinnati, OH 45220

Appendix Contents

I.	Appendix Materials and Methods.	Page 2
II.	Appendix Table S1.	Page 3
III.	Appendix Table S2.	Page 4
IV.	Appendix Table S3.	Page 5
V.	Appendix Figure S1.	Page 6
VI.	Appendix Figure S2.	Page 7
VII.	Appendix Figure S3.	Page 8
VIII.	Appendix Figure S4.	Page 9
IX.	Appendix References	Page 10

Appendix Materials and Methods

Immunostaining

To analyze proliferating LGR5⁺ stem cells, 5 μm frozen tissue sections were immunostained for GFP for 2 hr at room temperature, washed in 0.01% Triton X-100 in PBS (TPBS), and immunostained for Ki67 overnight at 4 °C. Appropriate secondary antibodies (1:400, Invitrogen) were applied for 30 min. at room temperature the following day, and sections were mounted with ProLong Gold containing 4,6-diamidino-2-phenylindole dihydrochloride (DAPI, Invitrogen). For Ki67 immunostaining, antigen retrieval was performed with Trilogy solution (Cell Marque, Rocklin, CA). For all other antibodies, antigen retrieval was performed with Antigen Unmasking Solution (Vector Laboratories, Burlingame, CA). Imaging by digital microscopy was done as previously described (Lopez-Diaz et al. 2006). To analyze goblet cell differentiation in *Lgr5; ROSA^{NICD}* mice, paraffin sections were immunostained for GFP as listed above. Visualization of GFP and Alcian Blue staining of goblet cells was performed as previously described (Carulli et al. 2015).

In situ hybridization

Lgr5 probes were made (DIG labeling kit, Roche) and purified (Mini-Elute Gel Extraction kit, Qiagen) according to manufacturer's instructions. Frozen sections were air-dried for 2 hours at room temperature and fixed in 4% PFA for 10 min. *Lgr5* probe was diluted in hybridization buffer (1:500) and incubated overnight at 68 °C. Tissue sections were washed, incubated in blocking solution in buffer (0.1M Maleic acid pH7.5, 0.15M NaCl, 0.1% Tween 20 in sterile H₂O) for 1 hr, and treated with anti-DIG antibody (1:2000, Roche) overnight at 4 °C. Slides were washed, developed and mounted with ProLong Gold.

I. Appendix Table S1. List of mouse strains and strain abbreviations used.

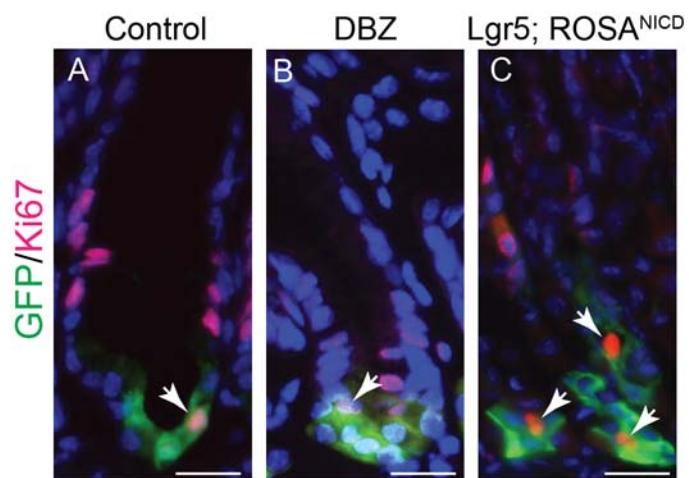
Mouse strains	Abbreviation
<i>NIP1::CreERT2; ROSA-LSL-EYFP</i>	<i>NIP1::CreERT2; ROSA^{EYFP}</i>
<i>Lgr5-EGFP-IRES-CreERT2; ROSA^{Notch1C}</i>	<i>Lgr5; ROSA^{NICD}</i>
<i>Bmi1-CreER; ROSA-CAG-LSL-tdTomato-WPRE; floxed-RBPJκ</i>	<i>Bmi1; ROSA^{Tom}; RBPJ^{f/+} or Bmi1; ROSA^{Tom}; RBPJ^{f/fl}</i>
<i>Lgr5-EGFP-IRES-CreERT2; ROSA-LSL-Confetti</i>	<i>Lgr5; ROSA^{Con}</i>
<i>Lgr5-EGFP-IRES-CreERT2; ROSA-LSL-Confetti; ROSA^{Notch1C}</i>	<i>Lgr5; ROSA^{Con}; ROSA^{NICD}</i>

II. Appendix Table S2. List of primary antibodies used for immunostaining.

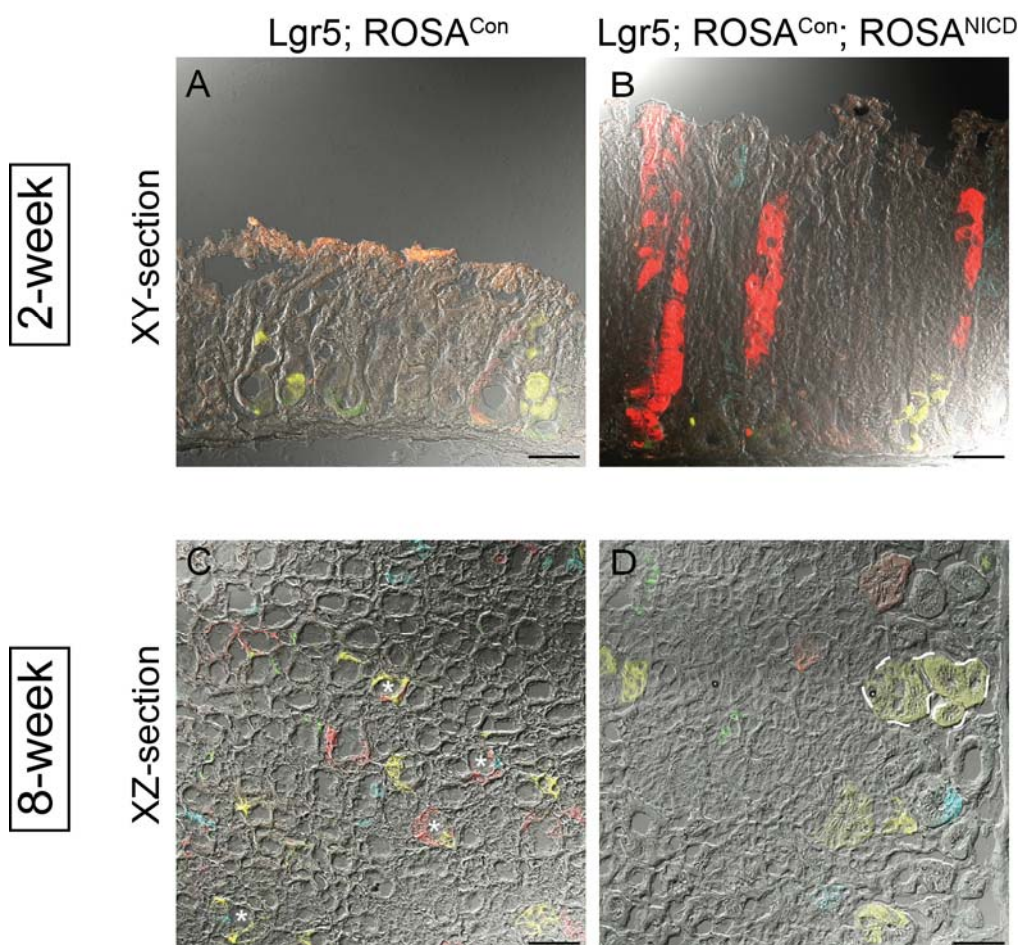
Antibody	Species	Source	Dilution	Reference
Anti-CD44	Rat	BD Pharmingen	1:50	(Qiao and Gumucio 2011)
Anti-E-cadherin	Rat	Invitrogen	1:1000	Figs 3 and 5
Anti-Gastrin	Rabbit	Dako	1:400	(Muller et al. 1987)
Anti-GFP	Chicken	Abcam	1:750	(Scopelliti et al. 2014)
Anti-GFP, 488 conjugate	Rabbit	Invitrogen	1:200	Figs EV4 and EV5
Anti-HES1	Rabbit	Abcam	1:50	(Dailey et al. 2013)
Anti-Ki67	Rabbit	Thermo Scientific	1:200	(VanDussen et al. 2012; Carulli et al. 2015)
Anti-Muc5AC	Mouse	Novacastra	1:75	(Keeley and Samuelson 2010)
Anti-pS6	Rabbit	Cell Signaling	1:300	Figs 9 and EV5
Anti-Sox9	Rabbit	Millipore	1:150	(VanDussen et al. 2012)
Anti-TFF2	Mouse	Abcam	1:100	(Keeley and Samuelson 2010)

III. Appendix Table S3. List of oligonucleotide sequences used for qRT-PCR.

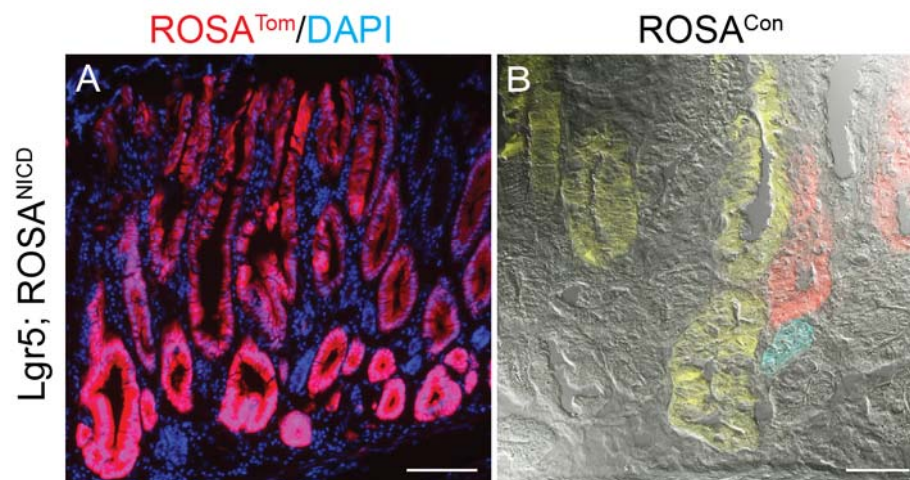
	Forward (5' to 3')	Reverse (5' to 3')	Amplicon Size (bp)
<i>Axin2</i>	AAGAGAAGCGACCCAGTCAATCC	GGTTCCACAGGCGTCATCTCC	278
<i>FoxQ1</i>	TGGCGGAGATCAACGAGTACC	CGCAGCACCTTGACGAAGC	121
<i>Gastrin</i>	GGACCAGGGACCAATGAGG	CCAAAGTCCATCCATCCGTAGG	173
<i>Hes1</i>	GCTCACTTCGGACTCCATGTG	GCTAGGGACTTTACGGGTAGCA	75
<i>Hey1</i>	GCCGACGAGACCGAATCAATAAC	CCCAAACCTCCGATAGTCCATAGCC	199
<i>Hey2</i>	ATTACCCTGGGCACGCTACAAG	GGCAAGAGCATGGGCATCAAAG	281
<i>HeyL</i>	AGAGACCGCATCAACAGTAGCC	TCAGTGAGGCATTCCCGAAACC	215
<i>Lgr5</i>	CGAGCCTTACAGAGCCTGATACC	TTGCCGTCGTCTTTATTCCATTGG	143
<i>Muc5ac</i>	GCCGTGTCCAGGAGTCTAATACC	CAGCCTAGCCACCACCTTCAG	133
<i>Muc6</i>	CCGGCGATGCAGCATGACTGG	CGCACTCCTGGTACACTTGGTTGG	101
<i>Neurog3</i>	ACCCTATCCACTGCTGCTTGTC	CGGGAAAAGGTTGTTGTGTCTCTG	136
<i>Olfm4</i>	GCCACTTTC AATTCAC	GAGCCTCTTCTCATAAC	199
<i>Spdef</i>	GGACGGACGACTCTTCTGACAG	GCTCCTGATGCTGCCTTCTCC	166
<i>Tf2</i>	TGCTTTGATCTTGATGCTG	GGAAAAGCAGCAGTTTCGAC	174



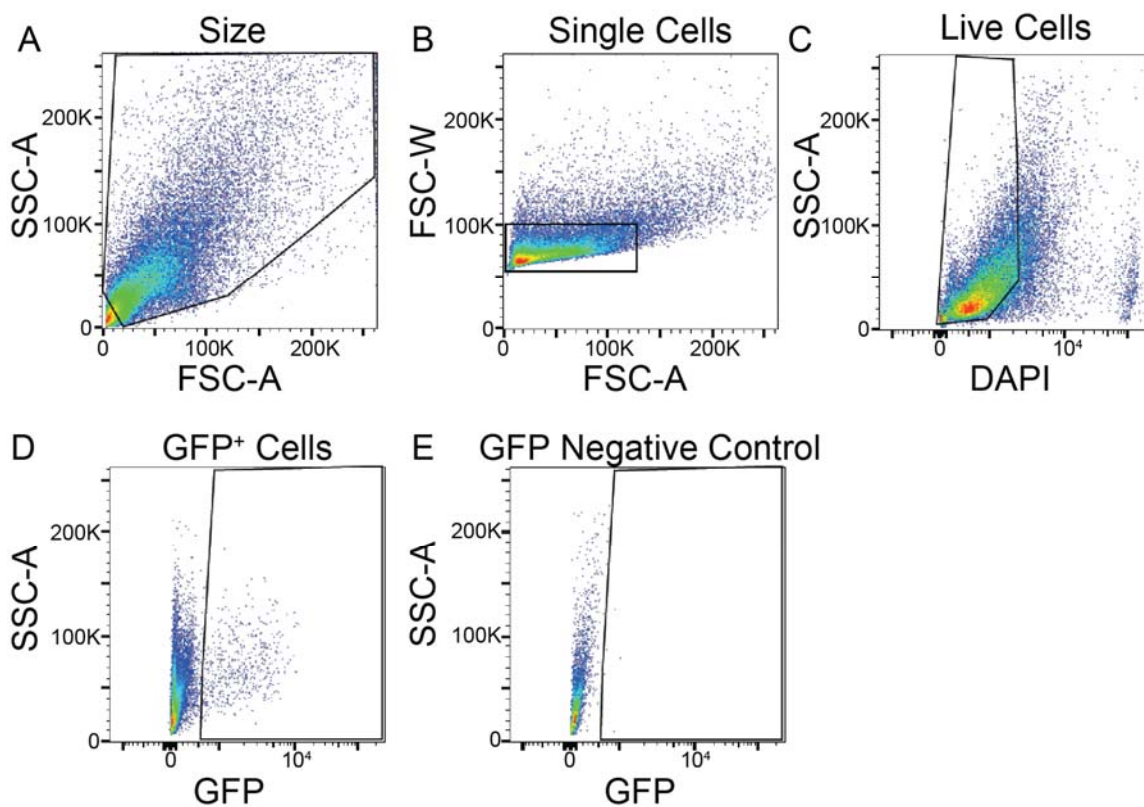
IV. Appendix Figure S1. Co-immunostaining for GFP/Ki67 in antral cryosections from (A) control, (B) DBZ or (C) *Lgr5; ROSA^{NICD}* 1 month post-TX. Arrowheads indicate GFP⁺/Ki67⁺ cells. Scale bars: 20 μ m.



V. Appendix Figure S2. (A&B) Analysis of *ROSA^{Con}* lineage tracing in *Lgr5*; *ROSA^{Con}* or *Lgr5*; *ROSA^{Con}*; *ROSA^{NICD}* antra 2-weeks post-TX. (C&D) Low-magnification view of XZ sections from *Lgr5*; *ROSA^{Con}* or *Lgr5*; *ROSA^{Con}*; *ROSA^{NICD}* antra 8-weeks post-TX. Asterisks in (C) indicate examples of polyclonal glands in control mice, whereas outlined glands in Notch-activated mice indicate a gland cluster (D). Scale bars: 50 μm.



VI. Appendix Figure S3. Lineage tracing in (A) *Lgr5*; *ROSA^{Tom}*; *ROSA^{NICD}* or (B) *Lgr5*; *ROSA^{Con}*; *ROSA^{NICD}* stomach 6 months post-TX. Scale bars: 50 μm.



VII. Appendix Figure S4. (A-D) Gating strategy for FACS sorting of single Lgr5-GFP⁺ antral stem cells for organoid initiation. The GFP⁺ gate was determined based on analysis of a non-transgenic negative control sample (E).

VIII. Appendix References

- Carulli AJ, Keeley TM, Demitrack ES, Chung J, Maillard I, Samuelson LC. 2015. Notch receptor regulation of intestinal stem cell homeostasis and crypt regeneration. *Dev Biol* **402**: 98-108.
- Dailey DD, Anfinson KP, Pfaff LE, Ehrhart EJ, Charles JB, Bonsdorff TB, Thamm DH, Powers BE, Jonasdottir TJ, Duval DL. 2013. HES1, a target of Notch signaling, is elevated in canine osteosarcoma, but reduced in the most aggressive tumors. *BMC veterinary research* **9**: 130.
- Keeley TM, Samuelson LC. 2010. Cytodifferentiation of the postnatal mouse stomach in normal and Huntingtin-interacting protein 1-related-deficient mice. *Am J Physiol Gastrointest Liver Physiol* **299**: G1241-1251.
- Lopez-Diaz L, Hinkle KL, Jain RN, Zavros Y, Brunkan CS, Keeley T, Eaton KA, Merchant JL, Chew CS, Samuelson LC. 2006. Parietal cell hyperstimulation and autoimmune gastritis in cholera toxin transgenic mice. *Am J Physiol Gastrointest Liver Physiol* **290**: G970-979.
- Muller J, Kirchner T, Muller-Hermelink HK. 1987. Gastric endocrine cell hyperplasia and carcinoid tumors in atrophic gastritis type A. *The American journal of surgical pathology* **11**: 909-917.
- Qiao XT, Gumucio DL. 2011. Current molecular markers for gastric progenitor cells and gastric cancer stem cells. *J Gastroenterol* **46**: 855-865.
- Scopelliti A, Cordero JB, Diao F, Strathdee K, White BH, Sansom OJ, Vidal M. 2014. Local control of intestinal stem cell homeostasis by enteroendocrine cells in the adult *Drosophila* midgut. *Current biology : CB* **24**: 1199-1211.
- VanDussen KL, Carulli AJ, Keeley TM, Patel SR, Puthoff BJ, Magness ST, Tran IT, Maillard I, Siebel C, Kolterud A et al. 2012. Notch signaling modulates proliferation and differentiation of intestinal crypt base columnar stem cells. *Development* **139**: 488-497.